RESEARCH PAPER

Formulation, Optimization and In-Vitro Assessment of a Montelukast Sodium-Loaded Proniosomal Gel for Sustained Drug Delivery in Asthma Management

Lalchand Devhare[1]*, Anitha K N[2], Kazi Sarfaraz Masoodali[3], Anita.A[4], Shobha A. Ubgade[5], Krishnakant B Bhelkar[6], Tufail Dana[7]

.

[1]*Nagpur College of Pharmacy, Wanadongri, Hingna Road, Nagpur, Maharashtra, India 441110*
[2]*Government College of Pharmacy, No 2, P Kalinga Rao Road, Subbaiah Circle, Karnataka, Bangalore 560027*
[3]*Fabtech College of Pharmacy, Sangola, Miraj-Pandharpur Road, Sangola Dist Solapur*
[4]*Dayananda Sagar University, Devarakagalahalli , Harohalli, Kanakapura Road 5602112*
[5, 6]*Gurunanak College of Pharmacy, Nari, Near Dixit Nagar, Kamptee Road, Nagpur*
[7]*Swami Vivekanand Sansthas Institute of Pharmacy, Mungase, Malegaon*

Received: 18th Aug, 2025; Revised: 26th Sep 2025; Accepted: 14th Nov, 2025; Available Online: 30th Nov, 2025

ABSTRACT

Montelukast Sodium is widely used for the management of asthma,but its low bioavailability due to the first-pass effect limits its therapeutic efficacy. A novel proniosomal gel-based delivery system can enhance EE, improve stability, and provide sustained drug discharge over an extended period.This study aims to formulate and assess a Montelukast Sodium proniosomal gel using different non-ionic surfactants, penetration enhancers, and gelling agents to optimize drug encapsulation, stability, and controlled drug discharge.Montelukast Sodium proniosomal gel was made using the coacervation phase separation approach. Varioussurfactants (Span 20/60/80, Tween 20/80), cholesterol (to control drug leakage), soya lecithin (as a penetration enhancer), and carbopol (as a gelling agent) were incorporated. The formulations were assessed for Fourier-transform infrared compatibility studies, vesicle size analysis, scanning electron microscopy (SEM), drug entrapment efficiency (EE), drug content, rheological behavior, in vitro drug discharge, and stability as per ICH Q1C guidelines.The study confirmed that Montelukast Sodium was successfully entrapped in all nine formulations. The type of surfactant and cholesterol content significantly influenced drug discharge and EE. FTIR analysis indicated no drug-excipient interactions, and SEM studies revealed uniform, spherical vesicles. The vesicle size of the optimized formulation (F2) ranged from 3.33±0.12 to 5.83±0.21 µm, with an EE of 54.46±0.50% and a drug discharge of 90.81±0.031%. The discharge kinetics followed a zero-order model and fitted the Higuchi equation, suggesting Super-Case II transport diffusion. Stability studies demonstrated that the formulation remained stable for 90 days, with the highest drug retention observed at 4°C.The optimized proniosomal gel formulation (F2) exhibited enhanced drug entrapment, prolonged drug discharge, and improved stability, making it a promising alternative for sustained delivery of Montelukast Sodium in asthma management.

Keywords: Montelukast Sodium, Proniosomal gel, Entrapment efficiency, Diffusion studies.

How to cite this article: Devhare L, N AK,Masoodali KS, A A,Ubgade SA,Bhelkar KB,Dana T, Formulation, Optimization, And In-Vitro Assessment of a Montelukast Sodium-Loaded Proniosomal Gel for Sustained Drug Delivery in Asthma Management. Int J Drug Deliv Technol. 2025;15(4): 1814-1825, DOI: 10.25258/ijddt.15.4.34

Source of support: Nil.

Conflict of interest: None

INTRODUCTION

Drug targeting is an advanced approach in pharmaceutical sciences that aims to distribute drugs specifically to the site of action, curtailing systemic side effects and surging drug efficacy. This strategy involves modifying drug molecules to achieve precise localization within the body, thereby improving therapeutic outcomes. Targeted drug delivery systems (DDS) can be passive/active/stimulus-responsive targeting[1]. Passive targeting relies on physiological conditions, such as the surge permeability and holding effect seen in tumor tissues, to accumulate the drug at the target site[2]. Active targeting involves modifying drugs with ligands that selectively bind to receptors amplified on infected cells. Stimuli-responsive targeting utilizes internal (pH, enzyme activity, redox potential) or external (temperature, magnetic field, ultrasound) activates to regulate drug discharge at the anticipated site[3]. Nanocarriers like liposomes, niosomes, dendrimers, and polymeric nanoparticles are usually used to facilitate drug targeting. These approaches improve drug bioavailability and therapeutic index and reduce toxicity, making them highly beneficial for treating diseases like cancer, inflammatory disorders, and neurodegenerative conditions[4].

Proniosomes are a promising nanocarrier system for targeted DDS, presentingrewards such as improved stability, precise drug discharge, and improved bioavailability. These are dry, free-flowing formulations

**Author for Correspondence: lalchand.devhare@gmail.com*

that, upon hydration, form niosomesvesicular structures containing non-ionic surfactants, cholesterol, and stabilizers[5]. Proniosomes are particularly useful for drug targeting as they encapsulate hydrophilic and lipophilic drugs, providing sustained and site-specific delivery[6]. They can be tailored for passive and active targeting by modifying their composition with ligands or surface modifications that enable receptor-mediated DDS. Due to their biocompatibility, proniosomes have been extensively studied for discharging drugs to cancer cells, inflammatory sites, and even across the blood-brain barrier. Additionally, their ability to enhance permeability through biological membranes makes them suitable for transdermal, oral, and pulmonary DDS[7]. Compared to conventional drug formulations, proniosomes exhibit improved therapeutic efficacy while minimizing systemic side effects, making them a valuable tool in modern drug-targeting strategies[8]. Montelukast is a selective leukotriene receptor antagonist (LTRA) widely used in the management of asthma and allergic rhinitis[9]. It works by blocking cysteinyl leukotriene receptors (CysLT1) in the airways, thereby reducing inflammation, bronchoconstriction, and mucus production[10]. This action helps prevent asthma attacks and alleviates symptoms [11]. Montelukast is usually prescribed as an oral tablet or chewable formulation, making it anexpedient option for long-term asthma control and exercise-induced bronchoconstriction[12]. Unlike corticosteroids, it does not cause significant immunosuppressive effects, making it suitable for chronic use, especially in pediatric and elderly populations. Additionally, Montelukast has shown potential in managing other inflammatory conditions, such as chronic urticaria and atopic dermatitis. Despite its effectiveness, it is not a rescue medication for acute asthma attacks and is usually used as an adjunct to inhaled corticosteroids or bronchodilators. Its good safety profile, ease of administration, and role in reducing asthma exacerbations make Montelukast a key drug in respiratory therapy[13].

The present research is to develop a proniosomal gel (PNG) system for Montelukast Sodium, to enhance *in vitro* bioavailability, certify ease of administration, improve patient compliance, and achieve a stable dosage formulation.

MATERIALS AND METHODS

Materials

Montelukast Sodium was gifted from Micro Labs Limited, Bengaluru, Karnataka, India. Soya lecithin, cholesterol, span 20,60,80, tween 20,80, carbopol 934P, triethanolamine, and ethanol used in the present work were of AR from S D Fine-Chem Limited, India.

Standard curve making

A precisely weighed 100 mg of Montelukast sodium was dissolved in phosphate buffer solution (PBS) (pH 7.4), and the volume was adjusted to 100 mL to form Stock A. From this solution, 10 mL was further diluted to 100 mL with the same PBS to obtain Stock B. Subsequently, a series of dilutions (10 to 40 µg/mL)wasmade to establish a calibration curve[14, 15]. The absorbance of these solutions was verified with a UV/Visible spectrophotometer at 283 nm.

Making of Proniosomes

The co-acervation phase separation tactic is one of the most used approachesfor preparing PNGs. In this process, surfactant, lecithin, cholesterol, and the drug are kept in a clean, dry, wide-mouthed glass vial (5mL). A specific volume of absolute ethanol (0.5–1 mL) is then added to the vial. The mixture is gently warmed and stirred using a glass rod to guarantee uniform dispersion. To prevent solvent evaporation, the vial is covered with a lid. The vial is then kept in a water bath at 65±2°C for approximately 5 minutes, allowing the surfactant mixture to dissolve totally. After this, 1.6 mL of PBS is introduced into the vial, and the mixture is further heated in the water bath for about two minutes until a clear solution is formed (Show in Fig.1). The solution is cooled to room temperature to get proniosomes[16].

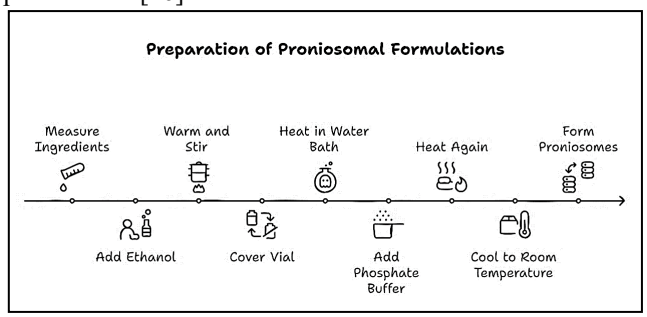

Fig.1. Preparation of proniosomal formulation

Making of Proniosomal gel

The required amount of Carbopol-934P was accurately weighed and allowed to soak in an appropriate volume of distilled water for 3 h. The mixture was then subjected to mechanical stirring at 100 rpm to obtain a homogeneous, viscous solution. To achieve neutralization, triethanolamine was added dropwise while incessantly stirring. Subsequently, additional excipients, including 0.2% methyl paraben and 0.02% propyl paraben, were incorporated into the mixture. Stirring was sustained until a clear, transparent gel was formed (Show in Fig.2). Finally, the proniosomes were thoroughly blended with the carbopol gel to certify uniform distribution.(Show in tabele.1) [17, 18].

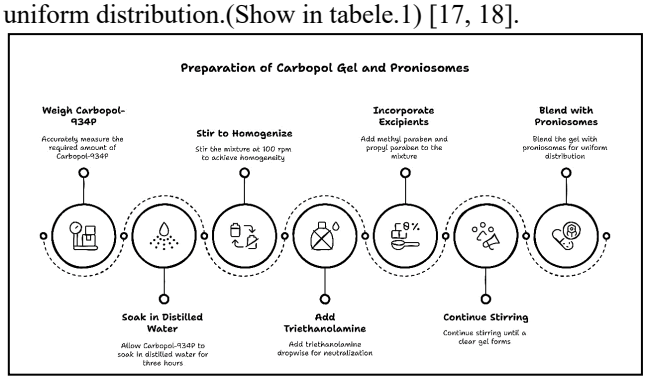

Fig.2. Step-wise representation of proniosomal gel making

Table1: Composition of proniosomal gels

Batch	Montelukast sodium (g)	Surfactants	Quantity (mg)	Cholesterol (mg)	Lecithin (mg)
F1	1	Span 20	1000	100	100
F2	1	Span 60	1000	100	100
F3	1	Span 80	1000	100	100
F4	1	Tween 20	1000	100	100
F5	1	Tween 80	1000	100	100
F6	1	Tween20:Tween80	500:500	100	100
F7	1	Span20: Span60	500:500	100	100
F8	1	Span60: Span80	500:500	100	100
F9	1	Span80: Span20	500:500	100	100

Assessing of proniosomal gel

Physical examination

The PNGs underwent a thorough visual inspection to assess their physical properties, which are crucial for ensuring their quality, stability, and patient acceptability[19]. The color was observed under both normal daylight and artificial lighting to certify uniformity and the absence of discoloration, as any unexpected changes could indicate instability, contamination, or ingredient incompatibility[20]. The odor was checked to confirm the absence of any unpleasant or rancid smell, as a neutral odor is desirable, and deviations may indicate degradation or microbial growth. Homogeneity was judged by visually inspecting and gently stirring the PNGs to certify uniform distribution of the active pharmaceutical ingredient (API) and excipients, which is essential for consistent drug discharge. The gel's consistency was assessed by touching and spreading a small amount between fingers to certify it had an optimal thickness, neither too thick nor too runny, allowing for easy application and effective DDS. The presence of grittiness was tested by rubbing the gel between fingers, as a smooth texture is essential for patient comfort and enhanced therapeutic action, while any coarse particles could indicate improper mixing, imperfect dissolution, or contamination. Spreadability was resolute by applying a verified quantity onto a glass slide and pressing it with another slide under constant weight, ensuring the gel spreads smoothly over the skin or mucosal surface without excessive force, as poor spreadability can lead to uneven drug distribution and reduced therapeutic efficacy. These physical features are vital in finding the PNG's effectiveness, patient compliance, and market acceptability, as any deviations in color, odor, consistency, or texture may signal instability that could compromise efficacy and safety. The outcomes of this comprehensive physical examination are systematically recorded and presented in Table 2, providing a clear assessment of the PNG's quality restrictions[21].

Assessing pH

The pH of the PNGs was assessed using a standardized pH meter to certify their compatibility with skin and mucosal surfaces, as an appropriate pH range is crucial to prevent irritation and maintain formulation stability. Before verification, the pH meter was adjusted using standard PBS to certify accuracy. A small quantity of each gel sample was dispersed in distilled water, and the electrode of the pH meter was immersed in the solution to obtain readings. Measurements were taken from three different samples to certify consistency and reliability, and the average pH was recorded. Maintaining an optimal pH is essential for enhancing patient comfort, ensuring drug stability, and preventing potential adverse reactions. Any significant deviation from the physiological pH range could lead to skin frustration or reduced therapeutic efficacy. The pH obtained for the PNGs is systematically documented in Table 3, providing insight into their suitability for intended pharmaceutical or dermatological applications[22].

Rheological studies

The viscosity of the PNGs (Brookfield viscometer) is used to find their flow behavior and certify consistency in application. Viscosity is a critical consideration that influences the gel's spreadability, retention on the skin, and overall therapeutic efficacy. To direct the measurement, a suitable spindle was selected based on the gel's consistency, ensuring accurate readings. The gel sample was transferred into a 30 mL beaker, taking care to prevent the entrapment of air bubbles, which could interfere with the viscosity measurements. The spindle was then engrossed appropriately in the gel, and the viscometer's motor was activated after inputting the spindle number. The viscosity was recorded using a floating-point display, providing precise measurements of the gel's resistance to flow[23]. The spindle selection was performed using a trial-and-error approach to optimize accuracy and certify reproducibility. Proper viscosity is indispensable for ease of use, patient comfort, and effective DDS.

Spreadability coefficient studies

The spreadability of the PNG was assessed 48 h post-preparation to assess its ease of use and uniform distribution over the skin or mucosal surface. This limit is crucial in finding the gel's ability to cover the intended area effectively without excessive effort. To direct the test, an adequate quantity of the gel was evenly applied to a clean, dry lower glass slide[24]. An identical upper glass slide was carefully positioned over the gel to certify uniform contact. A constant weight of 20 g was then kept on the upper slide and maintained for 2 h to standardize the pressure applied. The time required for the upper slide to slip off due to gravitational force was recorded, serving as an indirect measure of the gel's spreadability. A lower time reading designates better spreadability, which is essential for patient compliance and effective therapeutic action (e.q.1).

$$Spreadability = \frac{\text{Weight tied on upper slide (g)} \times \text{Length of glass slide (cm)}}{Time\ took\ (sec)} \text{--- (1)}$$

This estimation provides a quantitative measure of the gel's ease of application, ensuring that it meets the anticipated criteria for smooth and uniform[25].

SEM analysis

A small quantity (0.2 g) of the PNG was accurately weighed and diluted with 10 mL of PBS at pH 7.4 in a clean glass tube to facilitate vesicle dispersion. The resulting suspension was carefully made for Scanning Electron Microscopy (SEM) analysis to assess the morphological features, surface topology, and size distribution of the niosomal vesicles. The vesicles were equestrian onto an aluminum stub using double-sided adhesive carbon tape to confirm proper fixation. To enhance conductivity and improve imaging resolution, the vesicles were sputter-coated with a fine layer of gold-palladium (Au/Pd) using a vacuum evaporator. This coating prevents electron charging and allows for clearer visualization of the surface structure[26]. The coated vesicles were then analyzed under a SEM at an appropriate accelerating voltage, enabling high-magnification imaging of their surface features. The SEM marks provide critical insights into the vesicular morphology, structural integrity, and homogeneity of the PNGs.

Vesicle size analysis

To accurately determine the vesicle size (VS), 100 mg of the PNG was hydrated with a 0.9% saline solution in a small glass vial. The hydration process involved intermittent shaking for 10 minutes to guarantee uniform dispersion of the niosomal vesicles. The resulting suspension was then examined under an optical microscope at 100× magnification to visualize and measure the VS[27]. This analysis provided critical insights into the uniformity and size distribution of the vesicles, which are essential considerations influencing the stability and drug dischargefeatures of the PNGs.

Entrapment efficiency

To find theentrapment efficiency (EE) of the PNG, 0.1 g of the gel was reconstituted with 10 mL of PBS in a glass tube. The aqueous suspension was then subjected to sonication in a sonicator bath for 30 minutes to safeguard thorough dispersion of the niosomal vesicles. Following sonication, the montelukast-loaded niosomes were separated from the untrapped drug by centrifugation (10,000 rpm) at frozen conditions (4°C) for 30 minutes[28]. The supernatant was carefully collected, diluted with PBS, and analyzed spectrophotometrically at 283 nm using a UV-visible spectrophotometer. The % EE was estimated with e.q.2.

$$\% EE = \frac{\text{Total montelukast Sodium amount} - \text{Free montelukast Sodium amount}}{\text{Total montelukast Sodium amount}} \quad \text{--- (2)}$$

This analysis provided insights into the EE of the drug within the niosomal vesicles, which is a critical factor influencing drug discharge and therapeutic efficacy[25].

Drug content analysis

To assess the drug content, a quantity of proniosomes equivalent to 20 mg of Montelukast Sodium was transferred into a standard volumetric flask. The sample was lysed using 25 mL of methanol and subjected to unceasing shaking for 15 minutes to ensure complete dissolution of the drug. The resulting clear solution was then diluted to 100 mL with methanol to obtain a uniform level.

From this stock solution, a 10 mL aliquot was withdrawn and further diluted to 100 mL using PBS to maintain consistency in the analysis. The absorbance of the final solution was modulated at 283 nm using a UV-visible spectrophotometer. The amount of Montelukast Sodium was determined based on a previously established calibration curve, ensuring accurate quantification of the drug content in the PNGs[29].

***In vitro*diffusion**

The *in vitro* diffusion of the PNG were done with an egg/cellophane membrane to assess drug dischargefeatures. A quantity of PNG equivalent to 20 mg of Montelukast Sodium was carefully taken for the experiment. The membrane was securely equestrian onto a vertical Franz diffusion cell, ensuring that it faced the receiving chamber for proper diffusion.

The donor chamber was charged with the drug-containing PNGs, while the receiving chamber was filled with PBS to simulate physiological conditions. The membrane surface area accessible for diffusion was 2.54 cm², and the system was operated at 37 ± 0.5°C to replicate *in vivo* conditions. To certify uniform drug diffusion, the receptor fluid was unceasingly stirred at 100 rpm throughout the experiment[30].

At specific time points, 1 mL aliquots were removed from the receptor compartment and proximatelyswapped with an equivalent volume of fresh PBS to certify sink conditions were maintained[31]. The drug diffused was then quantified by UV-Vis spectrophotometry at a wavelength of 283 nm.

Kinetic modelling of drug dissolution outlines

The *in vitro* drug discharge profile of all PNGs was analyzed using various mathematical kinetic models to find the discharge mechanism. The data were plotted in different modes to assess the drug dischargefeatures. In the zero-order kinetic model, first-order, and Higuchi models [32]. Additionally, the Korsmeyer-Peppas model is used to find the discharge exponent (n), which helps classify the mechanism of transport. These kinetic models provide valuable insights into the dischargefeatures of the PNG, helping to understand the mechanism and control of drug discharge for enhanced therapeutic efficacy[33].

Stability studies

The optimized PNGs were sealed in 5 mL clear glass vials and subjected to stability studies under different storage conditions as per ICH Q1C guidelines. The PNGs were stored at 4°C and 25°C, and accelerated conditions (45±2°C and 75±5% RH) to assesstheir stability over time[34]. Samples were analyzed at specific intervals for physical

appearance, drug content, EE, and *in vitro* diffusion study for up to 90 days[34-49].

RESULTS

FTIR compatibilitystudies

The FT-IR spectroscopy analysis was directed to assess the compatibility of Montelukast Sodium with the selected polymers and excipients. The FT-IR spectrum of pure Montelukast Sodium exhibited distinct absorption peaks at 3399.10 cm^{-1} (COOH stretching), 2985.09 cm^{-1} (C-H stretching), 636.01 cm^{-1} (C-Cl stretching), 556.19 cm^{-1} (C-S stretching), 1588.50 cm^{-1} (C=C stretching), 1493.45 cm^{-1} (C-C stretching), and 3654.67 cm^{-1} (OH stretching). The FTR spectra of the physical mixture of Montelukast Sodium with excipients retained all typicalpeaks of the drug without significant shifts, disappearance, or formation of new peaks. This specifies that there was no major chemical contact between Montelukast Sodium and the excipients (Show in Fig.3).

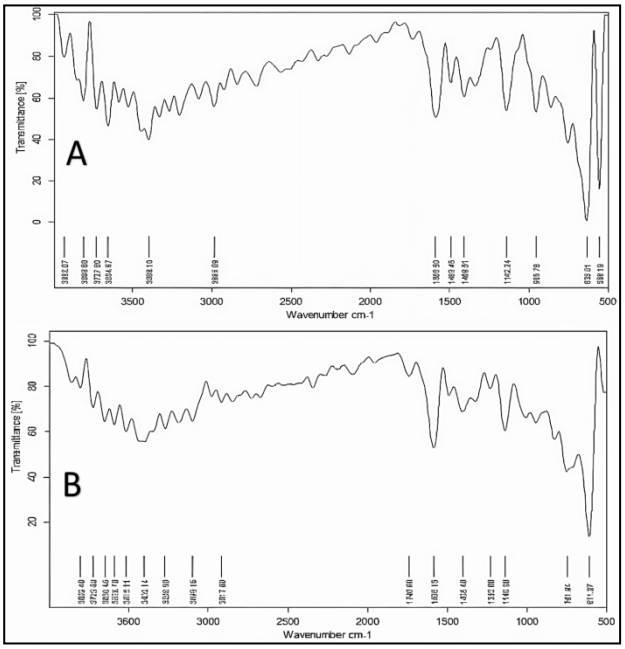

Fig.3. A) FTIR Spectrum of Montelukast Sodium & B) Along with all excipients

UV analysis of Montelukast

The absorption maximum (λ_{max}) of Montelukast Sodium was resolvedwith a UV-Visible spectrophotometer. The standard calibration curve of the drug was made in PBS by verifying the absorbance at the identified λ_{max}. The calibration curve displayed a straight-line relationship with a correlation coefficient (R^2) of 0.9969, demonstrating a strong linear correlation (Show in Fig.4).

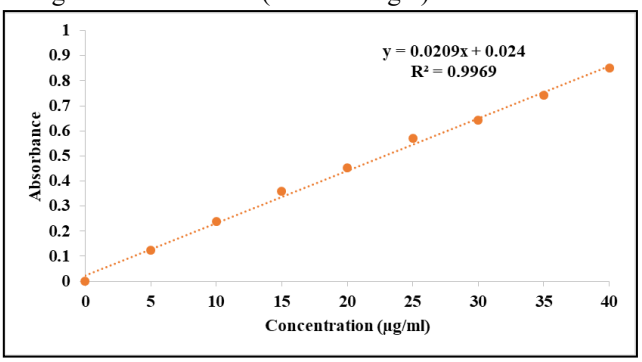

Fig.4. Calibration curve of Montelukast Sodium

Assessment

Physical examination

The PNG (F1–F9) were assessed for their physical properties, including spreadability, washability, homogeneity, color, odor, and phase separation. All PNGs demonstrated easy spreadability and were washable. They exhibited uniform homogeneity, appeared opaque in color, and had an aromatic odor. Additionally, no phase separation was observed in any of the PNGs (Show in Table 2).

Table 2: Physical examination of proniosomal gels

Trial	Spreadability	Washability	Homogeneity	Colour	Odour	Phase Separation
F1	Easy	Washable	Yes	Opaque	Aromatic	No
F2	Easy	Washable	Yes	Opaque	Aromatic	No
F3	Easy	Washable	Yes	Opaque	Aromatic	No
F4	Easy	Washable	Yes	Opaque	Aromatic	No
F5	Easy	Washable	Yes	Opaque	Aromatic	No
F6	Easy	Washable	Yes	Opaque	Aromatic	No
F7	Easy	Washable	Yes	Opaque	Aromatic	No
F8	Easy	Washable	Yes	Opaque	Aromatic	No
F9	Easy	Washable	Yes	Opaque	Aromatic	No

Determination of pH

The pH of the PNG was verified at 25ºC and found to be within the range of 6.74±0.178 to 7.20±0.134, which falls within the acceptable limits for topical preparations. The detailed pH for each PNGis presented in (Show in Table. 3).

Table 3: pH of proniosomal gels

Formulation	pH ± SD
F1	6.98 ± 0.054
F2	6.80 ± 0.043
F3	7.03 ± 0.167
F4	6.93 ± 0.068
F5	7.12 ± 0.231
F6	7.20 ± 0.134
F7	6.86 ± 0.125
F8	6.97 ± 0.202
F9	6.74 ± 0.178
Mean±SD; n=3	

Rheological studies

The rheological behavior of the PNG was judged by plotting a graph of shear rate vs. viscosity (Show in Fig.5). The results demonstrated that the viscosity of the PNGs reduced with an upsurge in shear rate, indicating a pseudoplastic flow. This behavior suggests that the PNGs exhibit non-Newtonian flow (shear-thinning properties), which is advantageous for topical application.

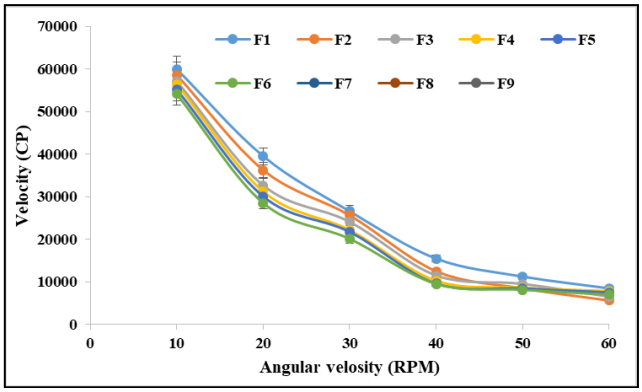

Fig.5. Rheological profile of proniosomal gels

Spreadability coefficient studies

The spreadability of different PNGs was assessed (Show in Table 4). All PNGs exhibited good spreadability, indicating ease of application. Among the tested PNGs, F4 demonstrated the highest spreading coefficient, suggesting superior Spreadability compared to the other PNGs.

Table 4: Spreadability of montelukast sodium gels

Trials	Time (sec)	Spreadability (gcm/sec)
F1	5.1±0.21	29.01 ± 0.32
F2	5.5±0.22	26.90 ± 0.25
F3	5.3±0.35	27.92 ± 0.43
F4	4.5±0.14	32.88 ± 0.47
F5	4.8±0.06	30.83 ± 0.06
F6	5.6±0.42	26.42 ± 0.17
F7	5.7±0.21	25.96 ± 0.24
F8	5.7±0.36	25.96 ± 0.08
F9	5.8±0.27	25.51 ± 0.36
Values in mean ±SD; n=3		

Vesicle size analysis

The VS is crucial for the topical application of vesicles, as it influences drug penetration and stability. The VS of the PNGsranged from 3.33 ± 0.12 to 5.83 ± 0.21 µm, as (shown in Fig.6.) Among the PNGs, F8 and F2, which were composed of span 60 and a grouping of span 20 and span 60, showed larger VS compared to the other PNGs.

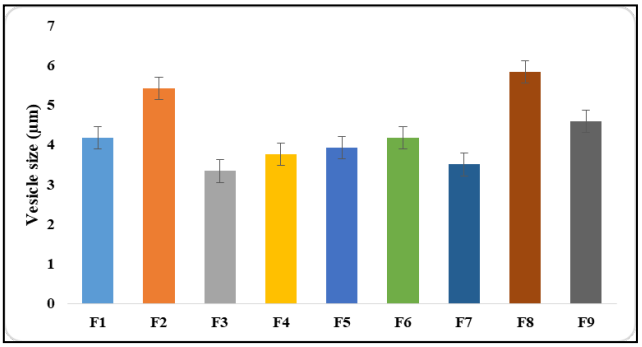

Fig.6. Comparison of vesicle size of proniosomal gels

Entrapment efficiency

The EE of the PNGs was found to range from 19.41 ± 0.89% to 54.46 ± 0.50%. The EE of all 9 PNGs is represented in Figure 7, with F2 exhibiting the highest EE (54.46%).

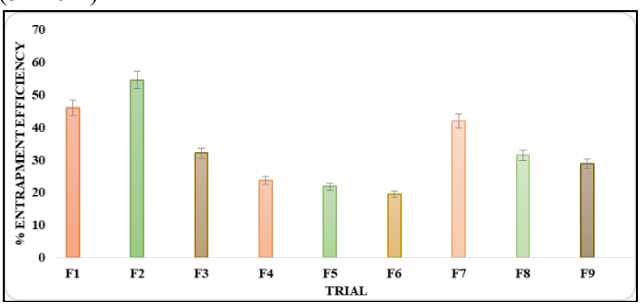

Fig.7. Comparison of the entrapment efficiency of proniosomal formulations

As shown in the result, proniosomes formed from span exhibited good EE. This could be clarifiedbased on the niosomal efficiency, which might be because of the leakage of the vesicles. The higher entrapment may be clarified by high cholesterol content.

Drug content analysis

The drug content of the developed PNGs(F1 to F9) containing Montelukast Sodium was found to be in the range of 90.22 ± 0.09% to 97.37 ± 0.19%, indicating a high level of drug loading within the PNGs. These readings suggest that the drug was effectively incorporated during the PNGs process and remained stable throughout the preparation.

SEM results

The SEM images of the optimized F2, as depicted in Fig.8, revealed that the vesicles are spherical with clearly defined and sharp boundaries. The vesicles appeared to be well-identified and distinguishable from one another, although there was slight heterogeneity in their size distribution.

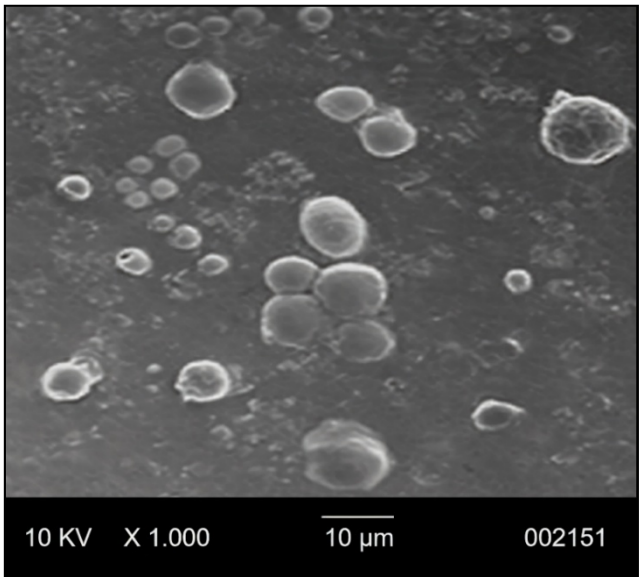

Fig.8. SEM analysis of F2

***In-vitro* diffusion studies**

The *invitro* drug diffusion study for Montelukast Sodium-loaded PNG was conductedover 12 h (Table 5). Among all the PNGs, F2 exhibited the highest drug discharge of 90.81% within 12 h. The initial phase of drug discharge (first 7 h) showed 40% to 50% discharge, which was likely due to the burst discharge of unstable or improperly formed niosomes. After 9 h, the discharge profile extending up to 12 h (Fig.9).

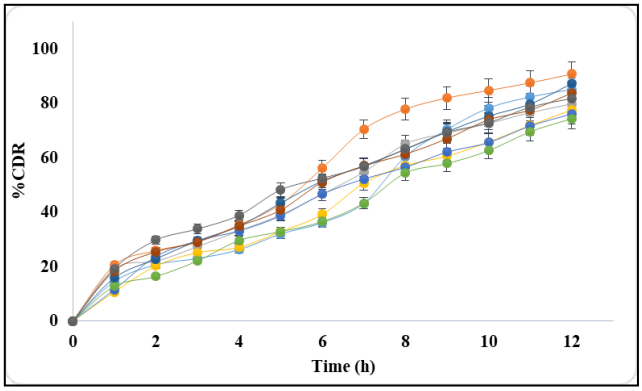

Fig.9. Drug discharge profile of the F1-F9

Drug discharge kinetics

The regression analysis for the *in vitro* drug discharge data of all PNGs was assessed using different kinetic models, as shown in Table 6. F2 exhibited the highest regression readings (R^2 = 0.9629) for Zero-order kinetics, indicating that drug discharge occurred at a constant rate, independent of concentration. The Higuchi model also showed a high regression coefficient (R^2 = 0.9412) for F2, suggesting that the discharge was diffusion-controlled. Furthermore, the Korsmeyer-Peppas model for F2 yielded an 'n' value of 1.1766, indicating Super case-II transport, which involves both diffusion and polymer relaxation mechanisms(Show in table. 5).

Table 5: Regression coefficient (r^2) values of kinetics model for the batches F1 to F9

Trial	Kinetic drug discharge		Mechanism of discharge		
	Zero order	First order	Higuchi	Korsmeyer-Peppas	
	R^2	R^2	R^2	R^2	Slope 'n'
F1	0.9689	0.6945	0.8756	0.7491	1.1906
F2	0.9629	0.6113	0.9412	0.6962	1.1766
F3	0.9782	0.6096	0.9545	0.6906	1.1258
F4	0.9899	0.6771	0.9384	0.7753	1.1980
F5	0.9796	0.6195	0.9384	0.7383	1.1645
F6	0.9919	0.6773	0.9348	0.7608	1.1638
F7	0.9892	0.6236	0.9646	0.7221	1.1724
F8	0.9825	0.5952	0.967	0.6846	1.1228
F9	0.9645	0.5506	0.9876	0.6524	1.0944

Stability studies data

The stability studies of the selected PNG were directed as per ICH Q1C guidelines over 90 days at different storage conditions: 4°C, 25°C, and 45±2°C with 75±5% RH. The PNGs were periodically assessed for visual appearance, pH, VS, EE, drug content, and *in vitro* diffusion studies, as presented in Table 6, Figures 10 and 11. The results demonstrated that the PNG remained most stable at 4°C, with no significant changes in physical or chemical features over the 12-week study period. The stability data of selected F2 stored at accelerated stability studies (45ºC±2 °C and 75±5% RH) is shown in Table 6.

Table 6: Physicochemical considerations of best F2 at 0, 1st and 2nd month

No. of days	Physical Appearance	pH	Vesicle size (µm)	%Drug content
0	No change	6.80±0.04	5.416±0.05	95.675±0.07
30	No change	6.74±0.06	5.833±0.07	95.563±0.08
60	No change	7.36±0.05	4.583±0.09	94.539±0.06
Value in mean±SD; n=3				

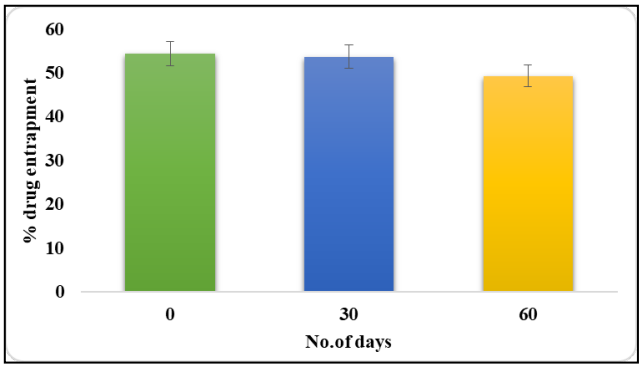

Fig.10. Drug entrapment of better formulation (F2) at 0, 1st, and 2ndmonths

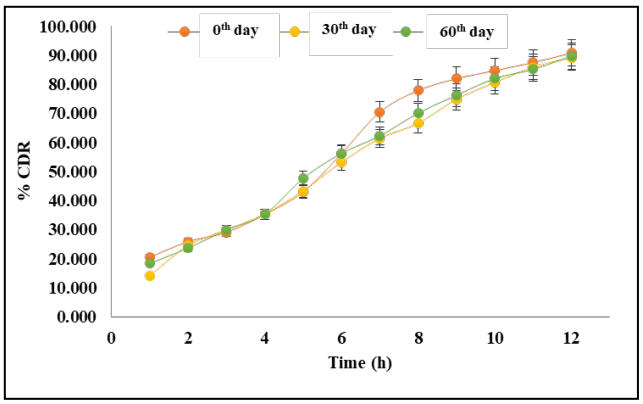

Fig.11 *In vitro* diffusion studies of best formulation F2 at 0, 1st, and 2nd months

DISCUSSION

FTIR spectroscopy is a reliable analytical tactic for detecting potential interactions between drug molecules and excipients in pharmaceutical formulations. In this study, the identical presence of functional group vibrations in both pure Montelukast Sodium and the physical mixture confirms that the molecular structure of the drug remains unchanged when combined with excipients. The absence of any significant peak shifts or additional peaks suggests that Montelukast Sodium remains chemically stable and compatible with the selected excipients. This is a crucial factor in ensuring the integrity and effectiveness of the final PNG. These findings support the suitability of the selected excipients for developing a stable proniosomal system for Montelukast Sodium.

The results confirm that Montelukast Sodium follows Beer's law in PBS, as indicated by the linearity of the calibration curve. The high correlation coefficient (0.9969) suggests an accurate and consistent relationship between drug levels and absorbance, ensuring precise quantification of the drug in further analytical and formulation studies. This validation supports the suitability of UV-visible spectrophotometry as a reliable tacticfor drug estimation.

The physical features of the PNG indicate its suitability for topical application. The absence of phase separation suggests good formulation stability, while the uniform homogeneity and ease of spreadability certify consistent application. The opaque appearance and aromatic odor contribute to user acceptability, further supporting the formulation's quality. These properties confirm that the gel meets essential criteria for an effective proniosomal DDS.

The observed physical features of the PNG suggest their suitability for topical application. The ease of spreadability certifys smooth application, while washability allows for convenient removal. Uniform homogeneity designatesthe proper distribution of ingredients, preventing inconsistencies in DDS. The opaque appearance and aromatic odor contribute to user acceptability, enhancing patient compliance. Moreover, the absence of phase separation confirms the stability of the formulations over the study period, making them suitable for further development.

The pH of a topical medications is a critical consideration that affects skin compatibility and overall stability. The observed pH indicates that the formulations are well within the physiological pH range of the skin, reducing the likelihood of exasperation or discomfort upon application. This guarantees that the PNGs are safe for prolonged use and maintain their effectiveness without causing adverse skin reactions.

The observed pseudoplastic behavior is desirable for topical medications as it confirms ease of application and spreadability on the skin. Non-Newtonian gels reduce resistance to flow under higher shear rates, meaning they become less viscous when applied and return to their original consistency when at rest. This property enhances user experience by facilitating smooth application while ensuring optimal retention on the skin after application. The findings confirm that PNGpossesses appropriate rheological properties for topical administration.

The ability of a topical medications to spread easily is a critical restriction influencing patient compliance and effectiveness. The high spreadability observed in formulation F4 suggests an optimal balance of viscosity and consistency, allowing for smooth application over the skin surface. The improved spreading coefficient of F4 could be attributed to the appropriate selection and levels of excipients, which facilitated better gel flow and distribution. This feature confirms uniform drug application, enhancing therapeutic efficacy.

VS plays a significant role in finding the stability and effectiveness of PNG. The results indicate that a surge in surfactant levels leads to a rise in VS, which could be due to the enhanced bilayer formation. However, an upsurge in EE resulted in a slash in VS, possibly due to better drug entrapment within the vesicular structure. The formulations with larger VS (F8 and F2) may offer sustained drug discharge, whereas those with smaller vesicles could facilitate better skin penetration. Thus, optimizing VS is essential for achieving the anticipated therapeutic outcome.

EE is a critical restriction in proniosomal formulations as it directly influences drug discharge and stability. The results indicate significant variability in EE across formulations, with F2 achieving the highest encapsulation (54.46%). This could be attributed to the optimized ratio of surfactants and cholesterol, which enhances drug incorporation within the vesicles. Higher EEguarantees improved drug retention,

leading to prolonged discharge and enhanced bioavailability. Variations in surfactant composition and levels may account for the observed differences among formulations. Thus, F2 may be a promising candidate for further development due to its superior drug retention capacity.

As shown in the results, proniosomes formulated using Span surfactants demonstrated good EE. This observation can be attributed to the ability of span surfactants, particularly span 60, to form stable vesicles with tight bilayer packing, which reduces drug leakage. The higher EE observed in some formulations may also be due to the augmented cholesterol content, which plays a key role in stabilizing the bilayer structure of vesicles. Cholesterol enhances membrane rigidity and reduces permeability, thereby minimizing drug leakage and contributing to improved entrapment. Therefore, the combination of span surfactants and high cholesterol levels appears to be a significant factor in achieving higher EE in proniosomal formulations.

The drug content analysis confirms that Montelukast Sodium was uniformly distributed across all the PNG. This uniformity is essential to certify consistency in therapeutic performance and reliable assessment in subsequent studies. The high % readings close to 100% also reflect the efficiency of the formulation approach and the compatibility of the drug with the excipients used. These drug content results provided the basis for estimating both EE and *in vitro* drug discharge, supporting the reliability and reproducibility of the developed PNG.

The SEM analysis confirmed the morphological features of the proniosomal vesicles. The spherical shape of the vesicles supports their potential for enhanced skin permeation and DDS. The slight heterogeneity in size may be attributed to the PNG making and surfactant composition, yet the sharp boundaries indicate good structural integrity of the vesicles. These morphological traits further validate the suitability of F2 for topical application and efficient drug entrapment.

The kinetic analysis of F2 confirms that the drug discharge follows Zero-order kinetics, which is a desirable characteristic for maintaining a consistent drug level over time. The strong correlation with the Higuchi model suggests that diffusion plays a significant role in drug discharge. The Korsmeyer-Peppas model results further reinforce that the discharge mechanism is Super case-II transport, meaning that in addition to diffusion, polymer swelling and relaxation also contribute to the controlled discharge profile. These findings highlight that F2 demonstrates an optimal balance between diffusion and matrix relaxation, making it a promising PNG for sustained DDS through PNG. The results suggest that the Zero-order kinetic model and Super case-II transport mechanism confirm a prolonged and controlled discharge of Montelukast Sodium, enhancing its therapeutic efficacy in topical applications.

The stability assessment revealed that lower storage temperatures (4°C) helped maintain the structural integrity of the vesicles, preventing aggregation or leakage of the drug. The pH, VS, EE, and drug content remained nearly unchanged at this temperature. However, at higher temperatures (25°C and 45±2°C), slight variations were observed, particularly in VS and EE, indicating minor degradation or instability over time. The *in vitro* diffusion profile of the PNG stored at 4°C showed consistent drug discharge, reinforcing the importance of storing proniosomal gels under refrigeration for better shelf stability. These findings suggest that temperature plays a crucial role in maintaining the efficacy and integrity of PNG, and storing them at lower temperatures is ideal for long-term stability.

CONCLUSION

The study successfully demonstrates the development of a stable and effective proniosomal gel (PNG) system for the topical delivery of Montelukast Sodium. FTIR analysis confirmed the absence of drug–excipient interactions, ensuring chemical stability. UV-spectrophotometric validation affirmed precise drug estimation, while the physical and rheological assessments supported the gel's suitability for skin application. Among all formulations, F2 emerged as the most promising, exhibiting optimal vesicle size, high entrapment, desirable spreadability, and a sustained zero-order drug release governed by Super case-II transport. Morphological analysis via SEM further validated the vesicular integrity, and stability studies emphasized the importance of cold storage for maintaining formulation quality. Overall, the findings establish F2 as a potent candidate for enhanced topical drug delivery, combining formulation stability with prolonged therapeutic efficacy..

.

REFERENCE

1. Reddy KTK, Reddy AS. Recent breakthroughs in drug delivery systems for targeted cancer therapy: an overview. Cellular, Molecular and Biomedical Reports 2025;5:13-27.
2. Alavi SE, Alharthi S, Alavi SZ, Raza A, Shahmabadi HE. Bioresponsive drug delivery systems. Drug discovery today 2024;29:103849.
3. Kang W, Xu Z, Lu H, Liu S, Li J, Ding C, et al. Advances in biomimetic nanomaterial delivery systems: harnessing nature's inspiration for targeted drug delivery. Journal of Materials Chemistry B 2024;12:7001-19.
4. Shang S, Li X, Wang H, Zhou Y, Pang K, Li P, et al. Targeted therapy of kidney disease with nanoparticle drug delivery materials. Bioactive Materials 2024;37:206-21.
5. Shehata TM, Ibrahim MM, Elsewedy HS. Curcumin niosomes prepared from proniosomal gels: In vitro skin permeability, kinetic and in vivo studies. Polymers 2021;13:791.
6. Teaima MH, Gebril MI, Abd Allah FI, El-Nabarawi MA. Niosomes versus proniosomes as promising drug

delivery systems in treatment of diabetes mellitus. Int J App Pharm 2022;14:32-40.
7. Nemr AA, El-Mahrouk GM, Badie HA. Development and evaluation of proniosomes to enhance the transdermal delivery of cilostazole and to certify the safety of its application. Drug development and industrial pharmacy 2021;47:403-15.
8. Shah H, Nair AB, Shah J, Jacob S, Bharadia P, Haroun M. Proniosomal vesicles as an effective strategy to optimize naproxen transdermal delivery. Journal of Drug Delivery Science and Technology 2021;63:102479.
9. Nayak A. A review of montelukast in the treatment of asthma and allergic rhinitis. Expert Opinion on Pharmacotherapy 2004;5:679-86.
10. Mayoral K, Lizano-Barrantes C, Zamora V, Pont A, Miret C, Barrufet C, et al. Montelukast in paediatric asthma and allergic rhinitis: a systematic review and meta-analysis. European Respiratory Review 2023;32.
11. Kim M-K, Lee SY, Park H-S, Yoon HJ, Kim S-H, Cho YJ, et al. A randomized, multicenter, double-blind, phase III study to evaluate the efficacy on allergic rhinitis and safety of a combination therapy of montelukast and levocetirizine in patients with asthma and allergic rhinitis. Clinical therapeutics 2018;40:1096-107. e1.
12. Krishnamoorthy M, Mohd Noor N, Mat Lazim N, Abdullah B. Efficacy of montelukast in allergic rhinitis treatment: a systematic review and meta-analysis. Drugs 2020;80:1831-51.
13. Pacheco Y, Freymond N, Devouassoux G. Impact of montelukast on asthma associated with rhinitis, and other triggers and co-morbidities. Journal of Asthma 2014;51:1-17.
14. Anant A, Saha M, Dhiman S, Singh P, Kurmi BD, Gupta GD, et al. An analytical review for the estimation of montelukast sodium. Separation Science Plus 2022;5:120-37.
15. Eldin AB, Shalaby AA, El-Tohamy M. Development and validation of a HPLC method for the determination of montelukast and its degradation products in pharmaceutical formulation using an experimental design. Acta Pharmaceutica Sciencia 2011;53:45-56.
16. Ahmed YM, Orfali R, Hamad DS, Rateb ME, Farouk HO. Sustainable release of propranolol hydrochloride laden with biconjugated-ufasomes chitosan hydrogel attenuates cisplatin-induced sciatic nerve damage in in vitro/in vivo evaluation. Pharmaceutics 2022;14:1536.
17. Baig RP, Wais M. Formulation and development of proniosomal gel for topical delivery of Amphotericin B. Int J Pharm Pharm Sci 2022;14:37-49.
18. Mohamed SA, Rofaeil RR, Salem H, Elrehany M, Asiri YI, Al Fatease A, et al. Proniosomal Gel-Loaded Phosphodiesterase Inhibitors (Sildenafil, Vardenafil, and Tadalafil): Prospects for Topical Penile Therapy of Tadalafil for Treatment of Erectile Dysfunction. Gels 2023;9:597.
19. Madan JR, Ghuge NP, Dua K. Formulation and evaluation of proniosomes containing lornoxicam. Drug delivery and translational research 2016;6:511-8.
20. Devi AS, Pinnika A, Divya P. Formulation and evaluation of candesartan cilexetil transdermal proniosomal gel. J Drug Del 2014;4:90-8.
21. Sandeep G, Devireddy SR. Formulation and evaluation of fluconazole pro-niosomal gel for topical administration. Journal of Applied Pharmaceutical Science 2014;4:098-104.
22. El-Emam GA, Girgis GN, El-Sokkary MMA, El-Azeem Soliman OA, Abd El Gawad AEGH. Ocular inserts of voriconazole-loaded proniosomal gels: formulation, evaluation and microbiological studies. International Journal of Nanomedicine 2020:7825-40.
23. Morteza-Semnani K, Saeedi M, Akbari J, Hedayati S, Hashemi SMH, Rahimnia SM, et al. Green formulation, characterization, antifungal and biological safety evaluation of terbinafine HCl niosomes and niosomal gels manufactured by eco-friendly green method. Journal of Biomaterials Science, Polymer Edition 2022;33:2325-52.
24. Alkilani AZ, Hamed R, Abdo H, Swellmeen L, Basheer HA, Wahdan W, et al. Formulation and evaluation of azithromycin-loaded niosomal gel: optimization, in vitro studies, rheological characterization, and cytotoxicity study. ACS omega 2022;7:39782.
25. Rezaei H, Iranbakhsh A, Sepahi AA, Mirzaie A, Larijani K. Formulation, preparation of niosome loaded zinc oxide nanoparticles and biological activities. Scientific Reports 2024;14:16692.
26. Farmoudeh A, Akbari J, Saeedi M, Ghasemi M, Asemi N, Nokhodchi A. Methylene blue-loaded niosome: preparation, physicochemical characterization, and in vivo wound healing assessment. Drug delivery and translational research 2020;10:1428-41.
27. Zaid Alkilani A, Hamed R, Abdo H, Swellmeen L, Basheer HA, Wahdan W, et al. Formulation and evaluation of azithromycin-loaded niosomal gel: optimization, in vitro studies, rheological characterization, and cytotoxicity study. ACS omega 2022;7:39782-93.
28. Ourani-Pourdashti S, Mirzaei E, Heidari R, Ashrafi H,

Azadi A. Preparation and evaluation of niosomal chitosan-based in situ gel formulation for direct nose-to-brain methotrexate delivery. International Journal of Biological Macromolecules 2022;213:1115-26.
29. Zhu L, Sun M, Wang L, Liu Y, Qu H. Preparation and evaluation of the curcumin niosomes: In vitro and in vivo. Pakistan Journal of Pharmaceutical Sciences 2023;36.
30. Temprom L, Krongsuk S, Thapphasaraphong S, Priperm A, Namuangruk S. A novel preparation and characterization of melatonin loaded niosomes based on using a ball milling method. Materials Today Communications 2022;31:103340.
31. Tyagi R, Waheed A, Kumar N, Ahad A, Bin Jardan YA, Mujeeb M, et al. Formulation and Evaluation of plumbagin-loaded niosomes for an antidiabetic study: Optimization and in vitro evaluation. Pharmaceuticals 2023;16:1169.
32. Ugorji OL, Umeh ONC, Agubata CO, Adah D, Obitte NC, Chukwu A. The effect of niosome preparation methods in encapsulating 5-fluorouracil and real time cell assay against HCT-116 colon cancer cell line. Heliyon 2022;8.
33. Jin Y, Liu D, Lu Z, Yang L, Chen J, Zhou X, et al. Preparation and evaluation of liposomes and niosomes containing total ginsenosides for anti-photoaging therapy. Frontiers in Bioengineering and Biotechnology 2022;10:874827.
34. Cetin EO, Salmanoglu DS, Ozden I, Ors-Kumoglu G, Akar S, Demirozer M, et al. Preparation of ethanol extract of propolis loaded niosome formulation and evaluation of effects on different cancer cell lines. Nutrition and cancer 2022;74:265-77.
35. Devhare LD, Anitha KN, Prasad KR, Lodhi GN, Umesh J, & Gote KB. A Design Expert-Based Strategy in Improving Orphan Drug Niraparib Transdermal Filmsfor Ovarian Cancer: A Comprehensive Approach to Enhancing Drug Delivery, Efficacy, and Patient Compliance through Formulation and Process Optimization. Journal of Applied Bioanalysis. 2025;11(5):179-190.
36. Devhare LD and Gokhale N. Antioxidant and Antiulcer Property of Different Solvent Extracts of Cassia Tora Linn. Research Journal of Pharmacy and Technology. 2022;15(3);1109-1113.
37. Tiwari R, Mishra J, Devhare LD and Tiwari G. An updated review on recent developments and applications of fish collagen. Pharma Times. 2023;55(6):28-36
38. Adimulapu AK, Devhare LD, Anasuya Patil A, Chachda NO, G. Dharmamoorthy. Design and Development of Novel Mini Tablet Cap Technology for the Treatment of Cardiovascular Diseases. International Journal of Drug Delivery Technology. 2023;13(3):801-806
39. Chawla A, Devhare LD, Dharmamoorthy G, Ritika, Tyagi S. Synthesis and In-vivo Anticancer Evaluation of N-(4-oxo-2- (4-((5-aryl-1,3,4 thiadiazole-2yl) amino) Phenyl thiazolidine-3-yl) Benzamide derivative. International Journal of Pharmaceutical Quality Assurance. 2023;14(3):470-474.
40. Gnana RPM, Devhare LD, Dharmamoorthy G, Khairnar MV, Prasidha R. Synthesis, Characterisation, Molecular Docking Studies and Biological Evaluation of Novel Benzothiazole Derivatives as EGFR Inhibitors for Anti-breast Cancer Agents. International Journal of Pharmaceutical Quality Assurance. 2023;14(3):475-480.
41. Sonule M, Devhare LD, Babu MN, Gunjal SD, Varalaxmi S. Microemulgel-based Hydrogel of Diclofenac Sodium using Lipidium sativum as a Gelling Agent. International Journal of Drug Delivery Technology. 2023;13(4):1235-1239.
42. Shriram BK, Devhare LD, Mehrotra A, Deokar SS, Singh SP. Formulation and Evaluation of Mosquito Repellent Stick. International Journal of Drug Delivery Technology. 2023;13(4):1283-1286.
43. Choudhary RK, Beeraka S, Sarkar BK, Dharmamoorthy G, Devhare L. Optimizing Verapamil Hydrochloride In-situ Delivery: A Strategic Formulation Approach using Box-Behnken Design for Enhanced Performance and Comprehensive Evaluation of Formulation Parameters. International Journal of Drug Delivery Technology. 2024;14(1):61-70.
44. Kumar KK, Kiran V, Choudhary RK, Devhare LD, Gunjal SD. Design Development and Characterization of Nicardipine Solid Lipid Nano-Particulars. International Journal of Drug Delivery Technology. 2024;14(1):71-78.
45. Priya MGR, Prasanth LML, Devhare LD, Yazdan SK, Gunjal S. Synthesis, DNA Binding, Molecular Docking and Anticancer Studies of Copper (II), Nickel (II), and Zinc (II) Complexes of Primaquine-based Ligand. International Journal of Pharmaceutical Quality Assurance. 2024;15(1):69-75.
46. Uplanchiwar VP, Raut SY, Devhare LD, et al. Pharmacological Assessment of Antiulcer Activity of Gloriosa Superba Linn Tubers In Experimentally Induced Gastric Ulcers. Journal of Medical Pharmaceutical and Allied Science. 2021;10(3);2852-2856.
47. Tiwari G, Gupta M, Devhare LD, & Tiwari R. Therapeutic and Phytochemical Properties of

Thymoquinone Derived from Nigella Sativa. Current Drug Research Reviews. 2024;16(2):145-156.

48. Chand, G., Devhare, L. D., & Hooda, T. . Diverse Properties of Tinospora Cordifolia (Giloy, Heart Leaved Moonseed) world wild use for immunotherapies;boosting the body's defence and immune support . Emerging Paradigms for Antibiotic-Resistant Infections: Beyond the Pill. Sringer Nature. 2024;1:471-486
49. Upreti, P., Devhare, L. D., Abdulmageed, L. H., Kumar, Y. G., Kumar, R., & Dharmamoorthy, G. Combatting Antibiotic Resistance: Leveraging Fecal Microbial transplantation for gut health. Emerging Paradigms for Antibiotic-Resistant Infections: Beyond the Pill. 2024;1:211-232

.